Journal of Alloys and Compounds 509 (2011) L236–L238

Contents lists available at ScienceDirect

Journal of Alloys and Compounds

journal homepage: www.elsevier.com/locate/jallcom

Letter

A facile method to prepare MoS_2 with nanolameller-like morphology

Tingting Yang[a], Xin Feng[a,b,*], Qingli Tang[b], Wenwen Yang[b], Jianhui Fang[a], Gangling Wang[b], Wen Shi[b], Liyi Shi[a,b,*], Peng Ding[b]

[a] Department of Chemistry, College of Science, Shanghai University, Shanghai 200444, PR China
[b] Nano Science and Technology Research Center, Shanghai University, Shanghai 200444, PR China

ARTICLE INFO

Article history:
Received 21 February 2011
Accepted 31 March 2011
Available online 8 April 2011

Keywords:
Nanostructures
Sulfides
Nanomaterials
Semiconducting materials

ABSTRACT

MoS_2 nanolamellers were synthesized by a one-step oxidation–reduction reaction in solution, in which the $(NH_4)_2MoS_4$ and $H_2C_2O_4{\cdot}2H_2O$ were used as reactants and then calcined at 800 °C under N_2 for 1 h. The products were characterized by X-ray diffraction (XRD), transmission electron microscopy (TEM), scanning electron microscopy (SEM), high-resolution transmission electron microscopy (HRTEM), X-ray photoelectron spectroscopy (XPS) and Raman spectroscopy. The diameter and nanoplate thickness of the obtained MoS_2 nanolamellers were approximately 80 nm and 20–30 nm, respectively. These novel structures of nanolamellers had potential applications in solid lubricants.

1. Introduction

Transition metal sulfides are a large family of materials that show many interesting functional properties. Therefore, they can be used in many fields, such as semiconductors, super conductors and fluorescent materials [1–3]. As a useful semiconductor, molybdenum disulfide (MoS_2) generally crystallizes with a hexagonal lamellar structure (S–Mo–S) and is composed of sulfur layers between which Mo atoms are inserted [4]. Each Mo atom is covalently bound to six sulfur atoms in a trigonal-prismatic coordination environment. The layers are held together by van der Waals's interactions between sulfur atoms. The lamellar-type structures make MoS_2 a useful solid lubricant for high vacuum applications [5], scanning probe microscopy [6], an intercalation host to forming new materials [7] and electrochemical hydrogen storage [8].

Recently, preparation of novel nanostructured MoS_2 and investigation of their electrochemical properties are attracting more and more attention. Various methods have been reported on the synthesis of nanosized MoS_2 [9–24], including the gas-phase reaction of MoO_3 and H_2S [10–12], thermal decomposition of ammonium thiomolybdate [13,14], and the solid-state reaction of $MoCl_5$ and Na_2S [15]. Sonochemistry, pulsed laser deposition, mechanochemical method, and hydrothermal reactions have also been developed to prepare nanosized MoS_2 at low temperature [16–25].

In this paper, we describe a simple and low-cost route to synthesize amorphous MoS_2 nanoparticles by oxidation–reduction reaction in aqueous solution, and the MoS_2 nanolamellars can be obtained by annealing amorphous MoS_2 in N_2 atmosphere. The interest in MoS_2 nanostructure is considered a focal at present. Herein, the synthesis route may offer an opportunity for fundamental studies and technological applications.

2. Experimental

The typical preparation procedure is as follows. First, 100 mL round-bottom flask was used to combine 70 mL deionized water. We heated it in a thermostat-equipped heating unit with magnetic stirring at 80 °C. Then 2.61 g $(NH_4)_2MoS_4$ and 1.26 g $H_2C_2O_4{\cdot}2H_2O$ were added to the flask, respectively. The reaction was kept at 80 °C for 1 h. The product was washed several times with ethanol and deionized water, then dried in vacuum at 80 °C for further processing.

The as-synthesized MoS_2 was subsequently dispersed on a quartz plate which was then located in the hot zone of the horizontal tube furnace. Prior to heating, N_2 gas at a flow rate of 200 cm^3 min^{-1} was kept flushing for about 0.5 h to remove residual air. The temperature of the furnace was increased gradually (10 °C/min) until 800 °C. The reaction temperature was hold in this temperature for 1 h. Finally, the product was cooled to room temperature gradually only under N_2 gas atmosphere. Then the final product was washed several times with ethanol and deionized water, then dried in vacuum at 80 °C.

The obtained products were characterized by following techniques. XRD patterns were recorded using Cu Kα radiation on a D/max-2500 difractometer. The morphology and structure were studied by SEM (JEOL JSM-6700F), TEM (JEOL JEM-200CX) and HRTEM (JEOL 3010 ARP). XPS were recorded on a Perkin-Elmer PHI-5300 spectrometer, using non-monochromatized Mg Kα radiation as excitation source in vacuum of 10^{-7} Pa. Raman spectra were taken under ambient conditions by using

* Corresponding author at: Department of Chemistry, College of Science, Shanghai University, Shanghai 200444, PR China. Tel.: +86 21 66136068; fax: +86 21 66136038.
E-mail addresses: fengxin@shu.edu.cn (X. Feng), shiliyi@shu.edu.cn (L. Shi).

0925-8388/$ – see front matter.
doi:10.1016/j.jallcom.2011.03.185

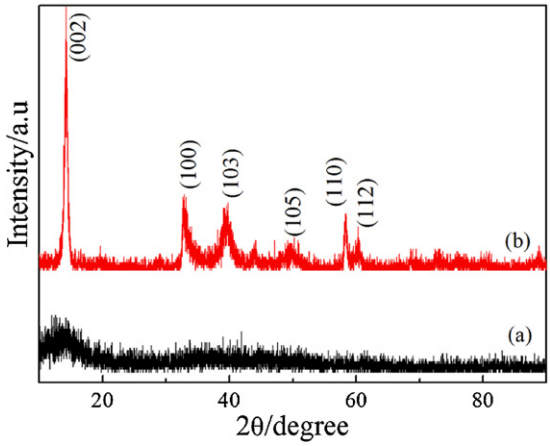

Fig. 1. XRD patterns of (a) the amorphous MoS_2 precursor and (b) the sample annealed at 800 °C in the atmosphere of N_2 for 1 h.

a Raman spectrometer (Almega Dispersive Raman, λ_{exc} = 532 nm). A glass substrate was used as the sample holder.

3. Results and discussion

The XRD patterns shown in Fig. 1 indicated that the crystallinity of the MoS_2 samples could be greatly improved by the annealing treatment. The above results indicate that the structures become more integrated and 2H–MoS_2 with characteristic peaks of (0 0 2), (1 0 0), (1 0 3), and (1 1 0) appears at the annealing temperature of 800 °C (indexing JCPDS file No. 37-1492). Fig. 1 confirms the presence of MoS_2 prepared from $(NH_4)_2MoS_4$ by the following oxidation–reduction reaction in aqueous solution:

$$(NH_4)_2MoS_4 + H_2C_2O_4 \rightarrow MoS_2 + 2CO_2 + 2H_2S + 2NH_3$$

As shown in Fig. 1, compared with the amorphous MoS_2 precursor, the annealed MoS_2 sample has a high and sharp diffraction

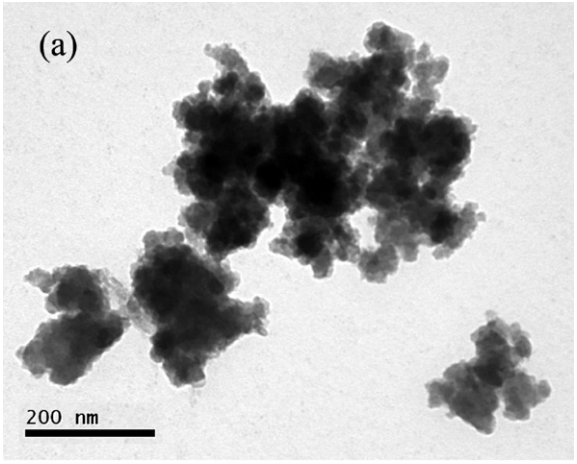

Fig. 2. TEM images of the samples of (a) the amorphous MoS_2 precursor and (b) the sample annealed at 800 °C in the atmosphere of N_2 for 1 h.

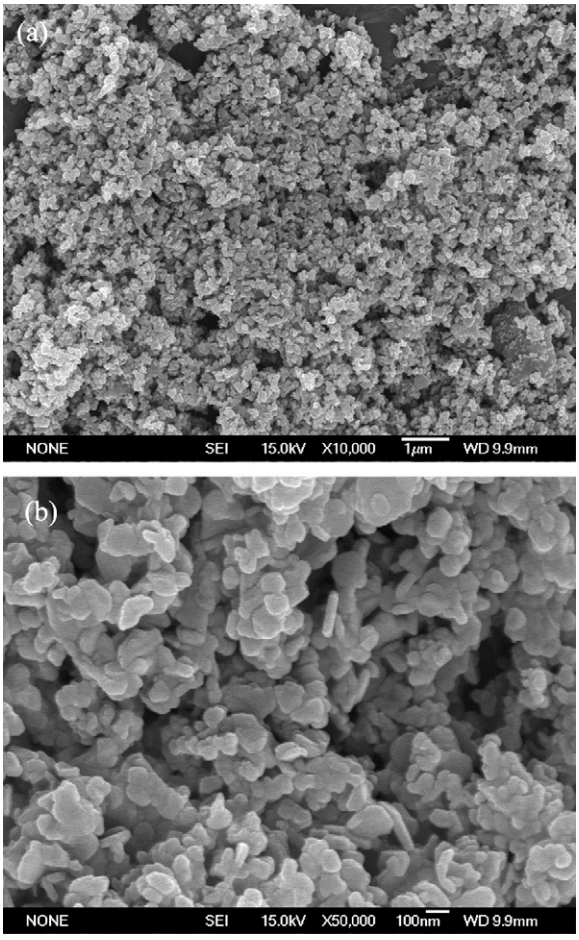

Fig. 3. SEM images of the sample annealed at 800 °C in the atmosphere of N_2 for 1 h.

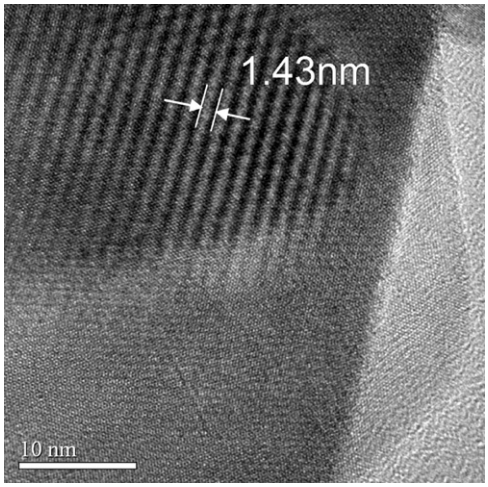

Fig. 4. HRTEM images of the sample annealed at 800 °C in the atmosphere of N_2 for 1 h.

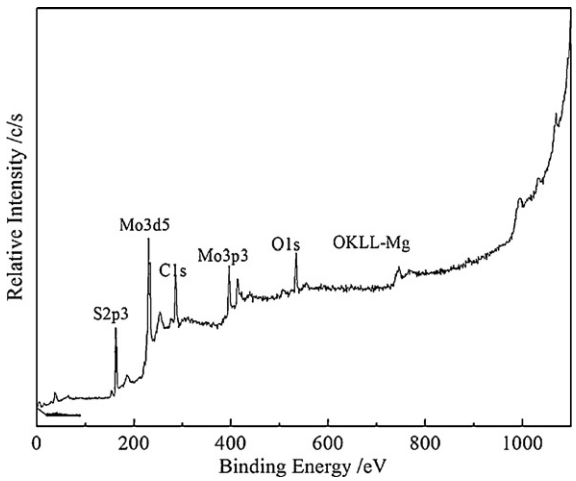

Fig. 5. X-ray photoelectron spectra of the sample annealed at 800 °C in N_2 atmosphere for 1 h.

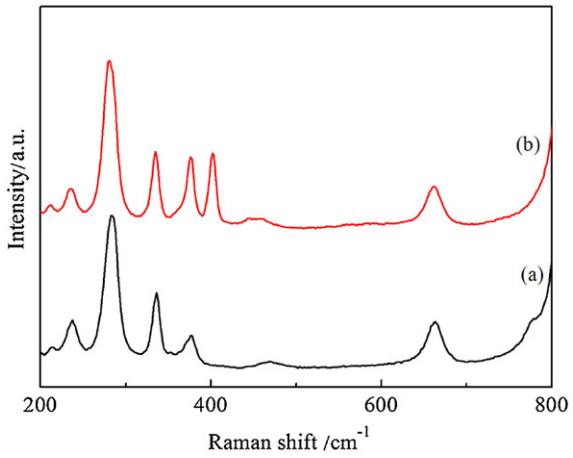

Fig. 6. Raman spectra of (a) the amorphous MoS_2 precursor and (b) the sample annealed at 800 °C in the atmosphere of N_2 for 1 h.

peak of (0 0 2), which indicates that the nanolamellar structure of MoS_2 formed during annealing treatment (Fig. 2(b)). The sample of annealed MoS_2 shows that it consists of homogeneous particles with an average diameter of ~80 nm. The high Gibbs free energy forces these particles to agglomerate and they are difficult to divide by an ultrasonic wave.

The typical SEM images are depicted in Fig. 3. The low-resolution SEM image (Fig. 3(a)) shows that the yield of nanolamellars is very high and more than 95%. Furthermore, the SEM image with high magnification (Fig. 3(b)) represents the morphology of nanolamellars. The SEM images further indicate that the obtained MoS_2 particles are aggregates with dimensions well below 100 nm. The plate thickness of the nanoplate structures is approximately 20–30 nm.

According to its HRTEM images (Fig. 4), the brim with a thickness of ~25 nm in the prepared nanolamellar MoS_2 particles at 800 °C annealed in the atmosphere of N_2 for 1 h presented obviously laminated structure with a little aberration. The approximately 1.43 nm lattice fringes correspond to the 2H–MoS_2 (0 0 2) layers.

A typical XPS spectrum of the sample annealed at 800 °C in the atmosphere of N_2 for 1 h is shown in Fig. 5, which indicates the presence of Mo, S, and unvoided surface contamination of C and O from absorbed gaseous molecules. The ratio of Mo/S calculated by measuring the areas of Mo and S cores is close to its chemical stiochiometry.

Typical Raman spectra of the unannealed and annealed MoS_2 samples are shown in Fig. 6. With the wavelength used, the data obtained were resonance Raman. Although the peak intensities had great difference, the unannealed and annealed MoS_2 had the analogous peak positions at about 405, 375, 350 and 280 cm^{-1}, consistent with the literature [24]. According to the literature [25] normal Raman peaks of MoS_2 appeared at about 380 and 408 cm^{-1}. In the resonance Raman spectrum, besides the enhancement of those peaks at 405 and 375 cm^{-1}, some new peaks at about 350 and 280 cm^{-1} were obtained. In the measurement, if the laser power was too large and focused on the sample for a long time, the MoS_2 sample would be partially oxidized and a peak at about 340 cm^{-1} might appear.

4. Conclusions

In summary, the amorphous MoS_2 was obtained by a one-step oxidation–reduction reaction in solution. Because of the rich sulfur bonds broken and the unsaturated bonds eliminated by controlling the annealing temperatures, MoS_2 with nanolamellar morphology can be obtained by annealing the amorphous MoS_2 in N_2 atmosphere. The nanolamellar MoS_2 has an average diameter of approximately 80 nm. The plate thickness of the nanoplate structures is approximately 20–30 nm. This paper may offer an easy way to prepare other metal sulfides nanolamellar particles.

Acknowledgements

This work was financially supported by Shanghai Nano-Science and Technology Special Project (0952nm01600), Innovation Program of Shanghai Municipal Education (09YZ22), Innovation Foundation of Shanghai University, and Project of Shanghai Municipal Science and Technology Commission (09dz1203902).

References

[1] B.T. Matthias, M. Marezio, E. Corenzwit, A.S. Cooper, H.E. Barz, Science 175 (1972) 1465–1466.
[2] P. Burlet, J. Flouquet, J.L. Genicon, R. Horyn, O. Pena, M. Sergent, Physica B 215 (1995) 127–133.
[3] D.N. Zheng, H.D. Ramsbottom, D.P. Hampshire, Phys. Rev. B 52 (1995) 12931–12938.
[4] J.K. Burdett, Chemical Bonding in Solids, Oxford University Press, New York, 1995.
[5] R. Tenne, M. Homyonfer, Y. Feldman, Chem. Mater. 10 (1998) 3225–3238.
[6] R. Rothschild, S.R. Cohen, R. Tenne, Appl. Phys. Lett. 75 (1999) 4025–4028.
[7] M. Danet, J.L. Mansot, A.S. Golub, G.A. Protzenko, P.B. Fabritchnyi, Y.N. Novikov, J. Rouxel, Mater. Res. Bull. 29 (1994) 833–841.
[8] J. Chen, N. Kuriyama, H.T. Takeshita, T. Sakai, J. Am. Chem. Soc. 123 (2001) 11813–11814.
[9] Y.D. Li, X.L. Li, R.R. He, J. Zhu, Z.X. Deng, J. Am. Chem. Soc. 124 (2002) 1411–1416.
[10] R. Tenne, L. Margulis, M. Genut, G. Hodes, Nature 360 (1992) 444–446.
[11] Y. Feldman, E. Wasserman, D.J. Srolovitz, R. Tenne, Science 267 (1995) 222–225.
[12] Y. Feldman, G.L. Frey, M. Homyonfer, V. Lyakhovitskaya, L. Margulis, H. Cohen, G. Hodes, J.L. Hutchison, R. Tenne, J. Am. Chem. Soc. 118 (1996) 5362–5367.
[13] C.M. Zelenski, P.K. Dorhout, J. Am. Chem. Soc. 120 (1998) 734–742.
[14] M. Nath, A. Govindaraj, C.N.R. Rao, Adv. Mater. 13 (2001) 283–286.
[15] P.R. Bonneau, R.F. Jarvis, R.B. Kaner Jr., Nature 349 (1991) 510–512.
[16] I. Bezverkhy, P. Afanasiev, M. Lacroix, Inorg. Chem. 39 (2000) 5416–5417.
[17] H.W. Liao, Y.F. Wang, S.Y. Zhang, Y.T. Qian, Chem. Mater. 13 (2001) 6–8.
[18] J.H. Zhan, Z.D. Zhang, X.F. Qian, C. Wang, Y. Xie, Y.T. Qian, J. Solid State Chem. 141 (1998) 270–273.
[19] K.M. Garadkar, A.A. Patil, P.P. Hankare, P.A. Chate, D.J. Sathe, S.D. Delekar, J. Alloys Compd. 487 (2009) 786–789.
[20] X.H. Chen, R. Fan, Chem. Mater. 13 (2001) 802–805.
[21] H. Lee, M. Kanai, T. Kawai, Thin Solid Films 277 (1996) 98–100.
[22] H. Li, W.J. Li, L. Ma, W.X. Chen, J.M. Wang, J. Alloys Compd. 471 (2009) 442–447.
[23] M.M. Mdleleni, T. Hyeon, K.S. Suslick, J. Am. Chem. Soc. 120 (1998) 6189–6190.
[24] Z.Z. Wu, D.Z. Wang, A.K. Sui, J. Alloys Compd. 492 (2010) L5–L7.
[25] G.W. Li, C.S. Li, H. Tang, K.S. Cao, J. Chen, F.F. Wang, Y. Lin, J. Alloys Compd. 501 (2010) 275–281.